

Enantioseparation and Amperometric Detection of Chiral Compounds by in Situ Molecular Imprinting on the Microchannel Wall

Ping Qu, Jianping Lei, Ruizhuo Ouyang, and Huangxian Ju*

Key Laboratory of Analytical Chemistry for Life Science (Ministry of Education of China), Department of Chemistry, Nanjing University, Nanjing 210093, P. R. China

The molecular imprinting technique was first introduced into the microchannel of a microfluidic device to form in situ the imprinted polymer for fast enantioseparation of chiral compounds. The molecularly imprinted polymer (MIP) was in situ chemically polymerized on the microchannel wall using acrylamide as the functional monomer and ethylene glycol dimethacrylate as the cross-linker, and characterized by scanning electron microscopy, atomic force microscopy, and infrared spectroscopy. Under the optimized conditions, such as optimal preparation of MIP, composition and pH of mobile phase, and separation voltage, the model enantiomers, *tert*-butoxycarbonyl-D-tryptophan (Boc-D-Trp) and Boc-L-Trp, could be baseline separated within 75 s. The linear ranges for amperometric detection of the enantiomers using carbon fiber microdisk electrode at +1.2 V (vs Ag/AgCl) were from 75 to 4000 μ M and 400 to 4000 μ M with the detection limits of 20 and 140 μ M, respectively. The MIP-microchip electrophoresis provided a powerful protocol for separation and detection of Boc-Trp enantiomers within a short analytical time. The molecular imprinting on microchannel wall opens a promising avenue for fast enantioscreening of chiral compounds.

Molecular imprinting technique (MIT) has become a well-known means for the preparation of biomimetic recognition matrices. The resultant materials have good binding affinity, stability, and specificity toward the target molecules, and thus have been widely applied in separation science,^{1–6} recognition of protein,^{7–9} biosensing,^{10–12} catalysis,¹³ and drug delivery.^{14–16} One of the most extensive applications of molecularly imprinted

polymer (MIP), an artificial receptor, is as chiral stationary phase for the separation of enantiomers in high-performance liquid chromatography (HPLC) and capillary electrochromatography (CEC). For example, a reversed-phase HPLC coupled with L-tetrahydropalmatine (THP)-imprinted monolithic precolumn has been developed for the determination of THP enantiomers,¹⁷ and a MIP nanoparticles-incorporated capillary has been used for CEC separation of drug enantiomers without apparent tailing.¹⁸ However, although a MIP-coated microchannel has been prepared,¹⁹ the enantioseparation and detection of chiral compounds using a microfluidic device have not been developed yet.

Microfluidic technology has been demonstrated to be a promising approach for various applications.^{20–27} Microchip electrophoresis (MCE) based on microfluidic devices has been one of the best candidates for fast microanalysis due to its small volume and portability. Generally, to achieve the separation of enantiomers in MCE, the chiral selector can be added in the mobile phase^{28–30} or immobilized as stationary phase.³¹ Two MCE

* Corresponding author. Phone/fax: +86-25-83593593. E-mail: hxju@nju.edu.cn.

- (1) Ou, J. J.; Li, X.; Feng, S.; Dong, J.; Dong, X. L.; Kong, L.; Ye, M. L.; Zou, H. F. *Anal. Chem.* **2007**, *79*, 639–646.
- (2) Spégel, P.; Schweitz, L.; Nilsson, S. *Anal. Chem.* **2003**, *75*, 6608–6613.
- (3) Wang, H. F.; Zhu, Y. Z.; Yan, X. P.; Gao, R. Y.; Zheng, J. Y. *Adv. Mater.* **2006**, *18*, 3266–3270.
- (4) Huang, Y. P.; Liu, Z. S.; Zheng, C.; Gao, R. Y. *Electrophoresis* **2009**, *30*, 155–162.
- (5) Jakschitz, T. A. E.; Huck, C. W.; Lubbad, S.; Bonn, G. B. *J. Chromatogr., A* **2007**, *1147*, 53–58.
- (6) Cacho, C.; Schweitz, L.; Turiel, E.; Pérez-Conde, C. *J. Chromatogr., A* **2008**, *1179*, 216–223.
- (7) Ouyang, R. Z.; Lei, J. P.; Ju, H. X. *Adv. Funct. Mater.* **2007**, *17*, 3223–3230.
- (8) Ouyang, R. Z.; Lei, J. P.; Ju, H. X. *Chem. Commun.* **2008**, 5761–5763.

- (9) Li, Y.; Yang, H. H.; You, Q. H.; Zhuang, Z. X.; Wang, X. R. *Anal. Chem.* **2006**, *78*, 317–320.
- (10) Tan, J.; Wang, H. F.; Yan, X. P. *Anal. Chem.* **2009**, *81*, 5273–5280.
- (11) González, G. P.; Hernando, P. F.; Alegria, J. S. D. *Biosens. Bioelectron.* **2008**, *23*, 1754–1758.
- (12) Henry, O. Y. F.; Piletsky, S. A.; Cullen, D. C. *Biosens. Bioelectron.* **2008**, *23*, 1769–1775.
- (13) Liu, J. Q.; Wulff, G. *J. Am. Chem. Soc.* **2008**, *130*, 8044–8054.
- (14) Zhu, Y. F.; Shi, J. L.; Shen, W. H.; Dong, X. P.; Feng, J. W.; Ruan, M. L.; Li, Y. S. *Angew. Chem., Int. Ed.* **2005**, *44*, 5083–5087.
- (15) Hilt, J. Z.; Byrne, M. E. *Adv. Drug Delivery Rev.* **2004**, *56*, 1599–1620.
- (16) Ansell, R. J. *Adv. Drug Delivery Rev.* **2005**, *57*, 1809–1835.
- (17) Ou, J. J.; Kong, L.; Pan, C. S.; Su, X. Y.; Lei, X. Y.; Zou, H. F. *J. Chromatogr., A* **2006**, *1117*, 163–169.
- (18) Wang, H. F.; Zhu, Y. Z.; Lin, J. P.; Yan, X. P. *Electrophoresis* **2008**, *29*, 952–959.
- (19) Lei, J. D.; Tong, A. J. *Spectrochim. Acta, Part A* **2005**, *61*, 1029–1033.
- (20) Zhan, Y. H.; Wang, J.; Bao, N.; Lu, C. *Anal. Chem.* **2009**, *81*, 2027–2031.
- (21) Liu, J. K.; Chen, C. F.; Tsao, C. W.; Chang, C. C.; Chu, C. C.; DeVoe, D. L. *Anal. Chem.* **2009**, *81*, 2545–2554.
- (22) Chung, K. H.; Crane, M. M.; Lu, H. *Nat. Methods* **2008**, *5*, 637–643.
- (23) Huang, B.; Wu, H. K.; Bhaya, D.; Grossman, A.; Granier, S.; Kobilka, B. K.; Zare, R. N. *Science* **2007**, *315*, 81–84.
- (24) Wu, D. P.; Qin, J. H.; Lin, B. C. *Lab Chip* **2007**, *7*, 1490–1496.
- (25) Tachi, T.; Kaji, N.; Tokeshi, M.; Baba, Y. *Anal. Chem.* **2009**, *81*, 3194–3198.
- (26) Zhao, S. L.; Li, X. T.; Liu, Y. M. *Anal. Chem.* **2009**, *81*, 3873–3878.
- (27) Zhai, C.; Li, C.; Qiang, W.; Lei, J. P.; Yu, X. D.; Ju, H. X. *Anal. Chem.* **2007**, *79*, 9427–9432.
- (28) Rodríguez, I.; Jin, L. J.; Li, S. F. Y. *Electrophoresis* **2000**, *21*, 211–219.
- (29) Piehl, N.; Ludwig, M.; Belder, D. *Electrophoresis* **2004**, *25*, 3848–3852.
- (30) Belder, D.; Ludwig, M.; Wang, L. W.; Reetz, M. T. *Angew. Chem., Int. Ed.* **2006**, *45*, 2463–2466.

methods have been successfully developed for high-speed chiral separation of amino acids by employing cyclodextrin derivatives as chiral selectors.^{28,29} A chip integrating a microfluidic reactor with chemical analysis has also been applied for online testing enantioselective biocatalytic products by adding a cyclodextrin derivative as chiral selector in the mobile phase.³⁰ An alumina gel-derived protein network formed on the microchannel has been prepared as a protein-stationary phase for on-chip analysis of chiral D- and L-tryptophan.³¹ This work introduced for the first time MIT into MCE for efficient enantioseparation of chiral compounds.

The separation and detection of *tert*-butoxycarbonyl-tryptophan (Boc-Trp) enantiomers are of importance in agriculture, food, and pharmaceutical industries since the chiral molecules as image and mirror image compounds show different physiological activity.^{32–34} Several HPLC methods for separation and detection of Boc-Trp enantiomers have been developed by packing Boc-L-Trp-imprinted particles into a stainless steel column.^{35–37} These methods are time-consuming (from 8 to 40 min) and have great consumption of reagents and samples, and packing MIP particles into the column is also inconvenient. By in situ molecular imprinting on microchannel wall using acrylamide (AM) as a functional monomer and ethylene glycol dimethacrylate (EDMA) as a cross-linker, the microfluidic device designed in this work could be used for fast separation of Boc-Trp enantiomers. This device integrated three polymer retainers with a MIP-coated quartz capillary for enantioseparation and a homemade carbon fiber microdisk electrode for amperometric detection. The resulting MIP-coated microchannel of microfluidic device (MIP-MCMD) achieved baseline enantioseparation of Boc-Trp within 75 s due to the large surface area and enough recognition sites on the wall of MIP-coated microchannel. In contrast to conventional molecular imprinting analysis, the designed MIP-MCMD showed fast separation and low reagent and sample consumption and had the potential to provide a facile platform for high-throughput screening of enantiomer candidates and donor–receptor interaction research.

EXPERIMENTAL SECTION

Materials and Reagents. Boc-D-Trp, Boc-L-Trp, AM, EDMA, and 3-(methacryloyloxy)propyltrimethoxysilane (γ -MPS) were all purchased from Alfa Aesar (Ward Hill, MA). 2,2'-Azobisisobutyronitrile (AIBN) was obtained from Acros (Geel, Belgium). HPLC-grade acetonitrile (ACN) and isooctane were supplied by Shanghai Chemical Reagent Co. (Shanghai, China). Fused-silica capillaries with an inner diameter (i.d.) of 25 μ m and outer diameter (o.d.) of 375 μ m were purchased from Yongnian Optic Fiber Plant (Hebei, China). Sylgard 184 silicone elastomer and curing agent were purchased from Dow Corning (Midland, MI). The running buffer and supporting electrolyte for MCE separation and amperometric detection were a mixture of ACN and acetic buffer solution (Nanjing Chemicals, Nanjing, China) filtered with a 0.2 μ m membrane. Stock solutions of Boc-Trp were prepared daily.

All aqueous solutions were prepared using ≥ 18 M Ω ultrapure water (Milli-Q, Millipore).

Equipment. A laboratory-built high-voltage power supplying controlled automatically by computer during experiments was used to supply separation voltage between 0 and +5000 V and sampling voltage between 0 and +1000 V, respectively. Electrochemical measurements were performed on a CHI 812 electrochemical station (CH Instruments Co.). For amperometric detection, a homemade carbon fiber microdisk working electrode (WE) was prepared as follows: a bundle of carbon fibers were inserted into a glass capillary (400 μ m o.d., 300 μ m i.d., and 2.5 cm length) and fixed by ethyl α -cyanoacrylate adhesive. After drying, graphite powder with a high purity was filled into the glass capillary from another end for contacting the carbon fibers with a copper wire (250 μ m diameter, 5 cm length), which was then inserted from this end and sealed in the capillary with epoxy resin for electric contact. The carbon fibers were ground on a fine sand paper to obtain the carbon fiber microdisk electrode. Prior to use, the surface of WE was polished on a finer sand paper and then rinsed thoroughly with doubly distilled water. The larger apparent diameter of the working electrode than the inner diameter of the separation channel led to an enhanced electrochemical response.

Ultrasonic disintegrator with a 2 mm o.d. probe from Ningbo Scientz Biotechnology (Ningbo, China) was used to prepare the sampling fracture on the separation capillary. An inverted fluorescence microscope (Nikon Eclipse TE2000-U) was used to observe the thickness of the MIP film on the inner wall of the capillary. A 40 multiple light microscope (Nanjing Optics Instruments Factory, Nanjing, China) was employed to monitor the position of the WE and detect the distance between the WE and the end of the separation microchannel. Scanning electron micrographs (SEM) were obtained with a Hitachi S-3000N scanning electron microscope (Japan) at an acceleration voltage of 10 kV. An atomic force microimage (AFM) was observed under an Agilent 5500 atomic force microscope. IR spectra were recorded on a Nicolet 400 Fourier transform-infrared (FT-IR) spectrometer (Madison, WI).

Preparation of the MIP-Coated Microchannel. A fused-silica capillary was flushed with 1 M NaOH followed by water for at least 30 min each. Then the capillary was silanized by filling a mixture of 4 μ L of γ -MPS and 1 mL 0.06 M acetic acid and keeping the mixture in the capillary for 1.5 h. The silanized capillary was then flushed with water and dried with a flow of nitrogen. The molar ratios of Boc-L-Trp, functional monomer (AM), and cross-linker (EDMA) used for the preparation of MIP for Boc-L-Trp were shown in Table 1. The optimized mixture for prepolymerization was composed of Boc-L-Trp (7.7 mg), AM (7.2 mg), EDMA (950 μ L), and initiator (AIBN, 1.0 mg) in 1.5 mL of ACN and 70 μ L of isooctane. At the same time, the thickness of MIP coating formed under different conditions was monitored. The mixture was first prepolymerized by sonication for 10 min and purged with dry nitrogen for 5 min to remove oxygen, then introduced to the capillary using a syringe. The ends of the capillary were sealed with soft plastic rubber. The capillary was submerged in a water bath for a certain time. After polymerization, the capillary was flushed using a hand-held syringe with ACN and methanol/acetic acid (9:1, v/v), respectively, to remove any unreacted reagent and

(31) Bi, H. Y.; Weng, X. X.; Qu, H. Y.; Kong, J. L.; Yang, P. Y.; Liu, B. H. *J. Proteome Res.* **2005**, *4*, 2154–2160.

(32) Kato, Y. J.; Kawakishi, S.; Aoki, T.; Itakura, K.; Osawa, T. *Biochem. Biophys. Res. Commun.* **1997**, *234*, 82–84.

(33) Ro, K. W.; Hahn, J. H. *Electrophoresis* **2005**, *26*, 4767–4773.

(34) Ludwig, M.; Kohler, F.; Belder, D. *Electrophoresis* **2003**, *24*, 3233–3238.

(35) Haginaka, J.; Kagawa, C. *Anal. Bioanal. Chem.* **2004**, *378*, 1907–1912.

(36) Yu, C.; Mosbach, K. *J. Mol. Recognit.* **1998**, *11*, 69–74.

(37) Yu, C.; Mosbach, K. *J. Org. Chem.* **1997**, *62*, 4057–4064.

Table 1. Conditions for Preparation of Boc-L-Trp-Imprinted Capillary

no. of capillary	T/M ^a	M/C ^b	T (°C)	time (h)	resolution
1	1:4	1:5	50	3.5	single peak
2	1:4	1:5	60	3.5	1.27
3	1:4	1:5	70	3.5	blocked
4	1:4	1:5	60	3.0	single peak
5	1:4	1:5	60	4.0	blocked
6	1:3	1:5	60	3.5	0.71
7	1:5	1:5	60	3.5	0.76
8	1:4	1:4	60	3.5	0.71
9	1:4	1:6	60	3.5	0.55
10	0:4	1:5	60	3.5	single peak

^a T/M: the molar ratio of template to functional monomer. ^b M/C: the molar ratio of functional monomer to cross-linker.

template. A nonimprinted polymer (NIP) modified capillary without imprinted molecules was prepared with a similar process.

Fabrication of Microfluidic Device. A detailed description on the fabrication procedure of the microfluidic device has been reported elsewhere.³⁸ Briefly, a poly(dimethylsiloxane) matrix with an inner channel of 375 μm diameter was obtained by pouring the mixture of Sylgard 184 silicone elastomer and curing agent into a mold and then divided into three segments as the polymer retainers for the preparation of sampling reservoir (SR), buffer reservoir (BR), and detection reservoir (DR), respectively. One as-prepared MIP-coated capillary (80 mm length) as the separation channel was inserted into the SR retainer until a small scratch made previously at the position of 8 mm from one end of the capillary appeared in the area of SR. After the BR and DR retainers were assembled to the two sides of the SR retainer by the capillary, the sampling fracture was obtained in the SR by sonicating the small scratch and the WE was mounted in the guide channel of the DR retainer, exactly opposite to the end of the separation channel at an optimum distance of $15 \pm 5 \mu\text{m}$. Then an Ag/AgCl reference electrode and a Pt wire as the auxiliary electrode were inserted to two sides of the DR to obtain an integrated three-electrode system for amperometric detection.

Enantioseparation of Chiral Compounds. The MIP-coated microchannel in the microfluidic device was first washed with methanol/acetic acid (9:1, v/v), which was filled in the BR and DR. The fracture sampling, a kind of sampling technology through the fracture into the separation channel,²⁷ was performed by applying an optimum injection voltage of 200 V between the SR and BR. The corresponding separation voltage was applied to the BR with the DR grounded and the SR floating by automatically switching the high-voltage contacts, and the electropherogram was recorded on a CHI 812 using the “amperometric $i-t$ curve” mode at an applied potential of +1.2 V, as shown in Figure 1. All experiments were performed at room temperature. Resolution was calculated with the equation $R_s = 1.18(t_L - t_D)/(W_{1/2,D} + W_{1/2,L})$, where t_D and t_L are the retention times of the enantiomers, respectively, and $W_{1/2,D}$ and $W_{1/2,L}$ are the peak widths of the enantiomers at the half peak height, respectively.

RESULTS AND DISCUSSION

Preparation of MIP-Coated Capillary. The MIP for Boc-L-Trp was in situ polymerized on the microchannel wall using AM

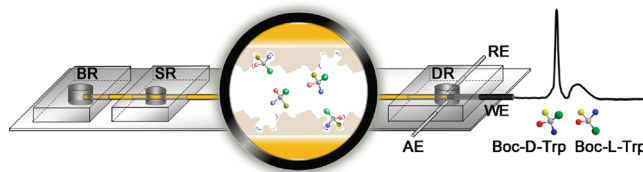


Figure 1. Schematic representation of enantioseparation of chiral compounds on MIP-MCMD. BR, buffer reservoir; SR, sample reservoir; DR, detection reservoir; WE, working electrode; RE, reference electrode; AE, auxiliary electrode.

as a functional monomer and EDMA as a cross-linker. In order to acquire a better performance, a series of MIP-coated capillaries were prepared according to the conditions listed in Table 1. The polymerization temperature and time played important roles in the formation of polymer. When the MIP-coated capillary was prepared with the polymerization time of 4 h at 60 °C (capillary 5), no solvent was flowing through the capillary even applying a separation voltage of 5000 V, indicating the blocked state of the capillary. When the polymerization time decreased to 3.5 h, the resulting capillary showed the largest resolution of 1.27 at 60 °C (capillary 2). It could be deduced that it was indeed possible to produce a three-dimensional imprinted polymer coat with controllable thickness on the capillary inner wall rather than blocking the capillary totally. However, a further decrease in the polymerization temperature or time led to the single peak (capillaries 1 and 4), which could be attributed to less imprinting recognition sites for the separation.^{1,39}

The molar ratios among the template, functional monomer, and cross-linker have been found to be important with respect to the number and quality of MIP recognition sites.^{17,40–45} When the ratio of template to functional monomer was 1:3 (capillary 6), the MIP-coated capillary showed high cross-reactivity for the Boc-Trp enantiomers due to the relatively similar structures of Boc-L-Trp and Boc-D-Trp. When the ratio was 1:5 (capillary 7), the MIP-coated capillary showed weak interaction due to the insufficient imprinting cavities. On the other hand, the amount of the cross-linker should be appropriate to not only maintain the stability of the recognition sites and the recognition cavities but also have some extent of the flexibility in order to make the template enter the cavities easily. At higher cross-linking degree (capillary 9), the recognition toward the template decreased because it was more difficult for the template to enter the cavities of the rigid MIP. When the cross-linking degree was lower (capillary 8), the column showed high cross-reactivity for Boc-D-Trp because the MIP skeleton had high flexibility, in which Boc-D-Trp entered the cavities easily. The optimal molar ratio of monomer to cross-linker was 1:5, at which the thickness of the imprinting film on the capillary inner wall was measured to be around 2.5 μm , and the

(39) Lin, L. Q.; Li, Y. C.; Fu, Q.; He, L. C.; Zhang, J.; Zhang, Q. Q. *Polymer* **2006**, *47*, 3792–3798.

(40) Yin, J. F.; Yang, G. L.; Chen, Y. J. *Chromatogr., A* **2005**, *1090*, 68–75.

(41) Huang, X. D.; Kong, L.; Li, X.; Zheng, C. J.; Zou, H. F. *J. Mol. Recognit.* **2003**, *16*, 406–411.

(42) Tan, Z. J.; Remcho, V. T. *Electrophoresis* **1998**, *19*, 2055–2060.

(43) Andersson, H. S.; Karlsson, J. G.; Piletsky, S. A.; Koch-Schmidt, A. C.; Mosbach, K.; Nicholls, I. A. *J. Chromatogr., A* **1999**, *848*, 39–49.

(44) Liu, X. J.; Ouyang, C. B.; Zhao, R.; Shangguan, D. H.; Chen, Y.; Liu, G. Q. *Anal. Chim. Acta* **2006**, *571*, 235–241.

(45) Liu, Z. S.; Xu, Y. L.; Yan, C.; Gao, R. Y. *J. Chromatogr., A* **2005**, *1087*, 20–28.

(38) Zhai, C.; Qiang, W.; Lei, J. P.; Ju, H. X. *Electrophoresis* **2009**, *30*, 1490–1496.

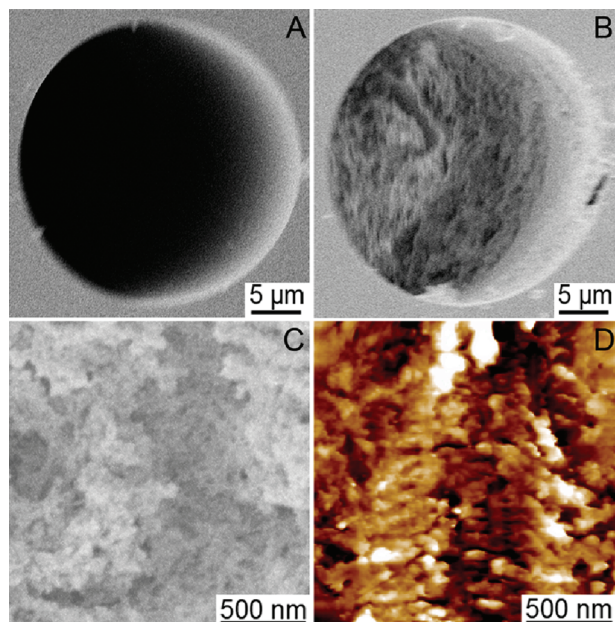


Figure 2. SEM images of (A) bare and (B) MIP-coated fused-silica capillaries and (C) SEM and (D) AFM images of the MIP-coated microchannel wall of MCMD.

MIP-coated microchannel showed good affinity and recognition toward the template Boc-L-Trp.

Characterization of MIP on Microchannel Wall. SEM image of the bare fused-silica capillary displayed a typical pillar structure with an inner diameter of 25 μm (Figure 2A). The morphology of the MIP-coated capillary was significantly different from that of bare capillary, since MIP covalently bound to the inner wall of capillary (Figure 2B). As shown in Figure 2C, the polymer film was highly porous and the skeleton linked to the inner wall of the MIP-coated capillary. An AFM image (Figure 2D) was used to confirm the surface morphology, which was consistent with that shown in Figure 2C. Thus, a three-dimensional imprinted porous polymer coat could be formed on the inner wall of the capillary under optimal conditions.^{46,47} The resultant open-tubular capillary was easily flushed by a low pressure, which facilitated fast regeneration and electrolyte exchange.

To ascertain the formation of MIP, FT-IR spectra of the cross-linker EDMA, the functional monomer AM, and the prepared MIP were compared in Figure 3. Two typical absorption peaks of primary amide of AM for N–H stretching vibration were observed at 3356 and 3184 cm^{-1} (Figure 3b). Compared with the spectrum of AM, the spectrum of MIP did not show the absorption peak at 3184 cm^{-1} (Figure 3c), suggesting the primary amide of AM became a secondary amide after polymerization. On the other hand, EDMA showed a small alkyl C–H stretching vibration at 2961 cm^{-1} (Figure 3a). After polymerization, the intensity of absorption at 2959 cm^{-1} was obviously enhanced, which could be attributed to the transduction from C=C in EDMA and AM to C–C in MIP. These results confirmed that MIP was successfully synthesized using AM as a functional monomer and EDMA as a cross-linker. However, from these FT-IR

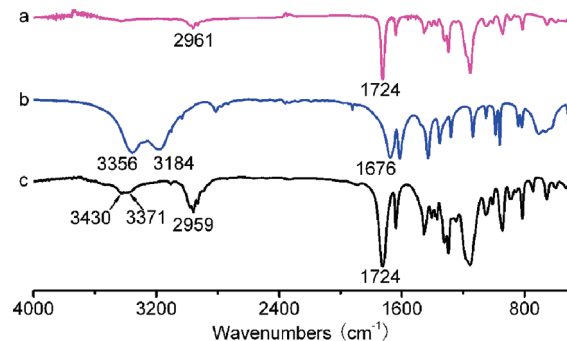


Figure 3. FT-IR spectra of (a) EDMA, (b) AM, and (c) MIP.

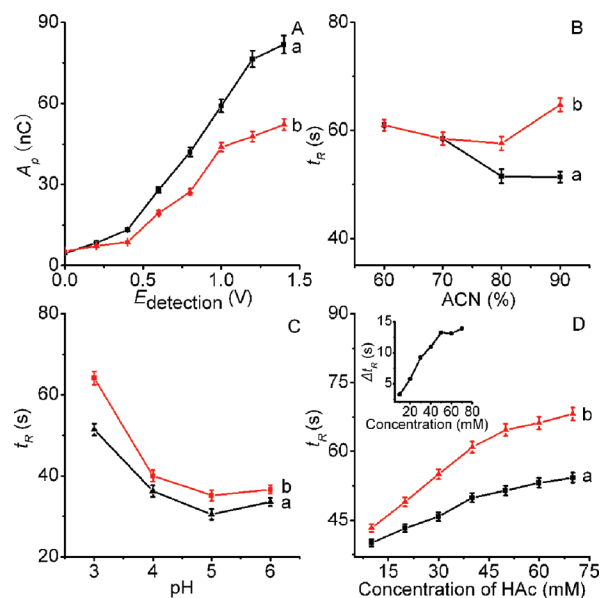


Figure 4. Effects of (A) the detection potential on peak area using ACN/50 mM acetate buffer (90/10, v/v, pH 3.0) as the running buffer and (B) ACN content, (C) pH of buffer, and (D) HAc concentration on retention time for 1 mM (a) Boc-D-Trp and (b) Boc-L-Trp at a detection potential of +1.2 V and separation voltage of 3000 V.

spectra, it was difficult to determine whether the template was removed after extraction due to the low concentration of the template in the as-synthesized polymer. To confirm the removal of the template after flushing, the UV–vis spectra of the eluants from MIP- and NIP-coated capillaries were compared (not shown). The eluant from the MIP-coated capillary showed higher UV–vis absorbance of Boc-Trp template at 282 and 290 nm than that from the NIP-coated capillary. These results confirmed the efficient elution of the template from the as-synthesized polymer.

Detection Potential. The electrochemical oxidation of Boc-Trp enantiomers at the carbon fiber microdisk electrode produced detectable amperometric signals. When the applied potential was less than +0.2 V, signals were very low. With the increase in the applied potential from +0.2 to +1.2 V, the amperometric responses increased, and a sharp increase occurred at the potentials more positive than +0.4 V (Figure 4A). When the applied potential was higher than +1.2 V, the oxidation current increased slowly, which was due to the high oxidation potential resulting in a very noisy and unstable baseline.⁴⁸ Therefore, +1.2 V was used as the

(46) Brüggemann, O.; Freitag, R.; Whitcombe, M. J.; Vulfson, E. N. *J. Chromatogr., A* **1997**, 781, 43–53.

(47) Xie, C. H.; Hu, J. W.; Xiao, H.; Su, X. Y.; Dong, J.; Tian, R. J.; He, Z. K.; Zou, H. F. *Electrophoresis* **2005**, 26, 790–797.

(48) García, C. D.; Henry, C. S. *Anal. Chem.* **2003**, 75, 4778–4783.

optimum detection potential, at which the broader peak shape for the imprinted L-enantiomer, as observed in enantioseparation,^{1,17,36} made accurate integration more difficult. However, this did not affect the quantitation of Boc-L-Trp.

Optimization of the Mobile Phase. The effects of ACN content in the mobile phase on the retention times of Boc-D-Trp and Boc-L-Trp were shown in Figure 4B. In the ACN concentration range of 60–80%, with increasing ACN content both retention times decreased due to the increasing electroosmotic flow (EOF) mobility⁴⁵ and the relatively weak hydrophobic interaction at high acetic acid concentration. When the ACN concentration was higher than 80%, the hydrophobic interaction was enhanced, thus the retention time of Boc-D-Trp in the Boc-L-Trp-imprinted MCMD increased gradually and the specific recognition of Boc-L-Trp-imprinted MCMD for the template led to a sharply increased retention time of Boc-L-Trp. Considering the retention and the resolution, an ACN content of 90% (v/v) in the mobile phase was chosen for following experiments.

The effect of pH on the retention was studied from pH 3.0 to 6.0 (Figure 4C). With the increase of pH, the retention trend of Boc-Trps on MIP-MCMD decreased due to the increase of EOF. It was worth noting that the retention time of Boc-Trps at pH 6.0 increased, which might be contributed to a stronger interaction between MIP and the Boc-Trps when pH was higher than the pK_a value of the imprinted molecule (pK_a of Boc-L-Trp is 4.5).

Figure 4D shows the effect of salt concentration on the retention of Boc-Trp enantiomers on the Boc-L-Trp-imprinted capillary. With the increase of salt concentration, both the retention times (t_R) of Boc-D-Trp and Boc-L-Trp increased, and the difference of t_R (Δt_R) increased and reached a plateau at the concentration of 50 mM. It further identified the retention was controlled by a hydrogen-bonding interaction mechanism at high ACN content.

Sampling Conditions and Separation Voltage. The effect of sample loading on separation was studied by electrokinetic injection with application of different sampling voltages and times, and an optimum injection voltage of 200 V at the injection time of 2 s was selected for obtaining good separation efficiency and appropriate detection sensitivity. As the sample loading increased, the retention time of the analyte increased and the resolution reduced sharply. These phenomena were similar to that in HPLC and may be attributed to the limited number of recognition sites on the MIP-coated inner wall of the microchannel.

The effect of separation voltage was investigated on the Boc-L-Trp-imprinted MCMD (Figure 5). The separation time was greatly shortened from 200 to 75 s with the increase of separation voltage from 1000 to 3000 V, meanwhile, the resolution increased due to the narrow broadening of signal. In contrast, at the higher separation voltages, the resolution decreased. At 3000 V, the baseline separation of Boc-Trp enantiomers was successfully acquired within 75 s on the Boc-L-Trp-imprinted MCMD with the largest resolution of 1.27. Compared with those obtained from conventional molecularly imprinted HPLC analysis,^{35–37} the separation time obtained from the MIP-MCMD was much shorter than 8–40 min.

Separation Efficiency of Enantiomers. The separation efficiencies of Boc-D-Trp and Boc-L-Trp on MIP-, NIP-, and bare

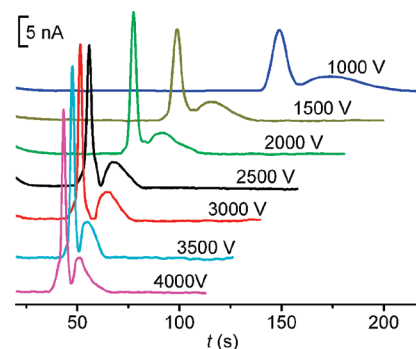


Figure 5. Effect of separation voltage on the enantioseparation of 1 mM Boc-D-Trp and Boc-L-Trp using ACN/50 mM acetate buffer (90/10, v/v, pH 3.0) as the running buffer at a detection potential of +1.2 V.

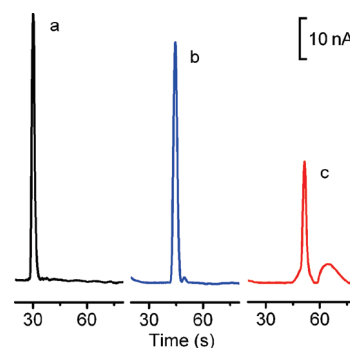


Figure 6. Separation of Boc-D-Trp and Boc-L-Trp in (a) bare, (b) NIP-, and (c) MIP-coated capillaries of MCMD using ACN/50 mM acetate buffer (90/10, v/v, pH 3.0) as the running buffer at a detection potential of +1.2 V and separation voltage of 3000 V.

MCMD were shown in Figure 6. Boc-Trp enantiomers could not be separated on both the NIP- and bare capillary at all (electropherograms a and b in Figure 6) due to the absence of recognition sites complementary to the spatial structure of Boc-L-Trp. On the MIP-MCMD (electropherogram c in Figure 6), baseline separation was achieved with the resolution of 1.27. This result could be attributed to sufficient recognition sites on the inner wall of the capillary for the separation of Boc-Trp.

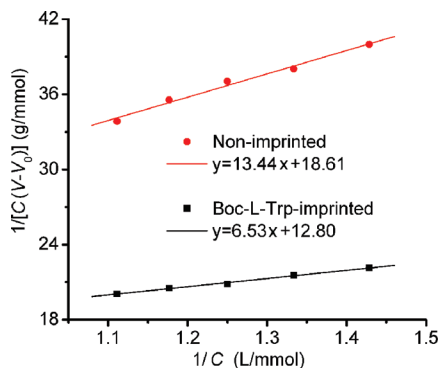
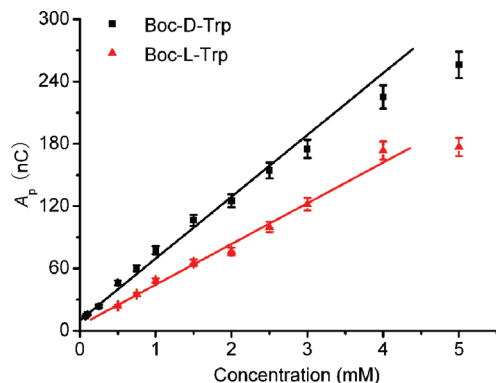
Binding Capacity. Frontal chromatography can be used for characterization of specific interaction in MIP-based system according to⁴⁴

$$\frac{1}{C(V - V_0)} = \frac{K_d}{CL_t} + \frac{1}{L_t} \quad (1)$$

where C is the concentration of analyte, V and V_0 are the elution volumes of the analyte and the void marker, respectively, L_t is the effective number of binding sites, and K_d is the dissociation constant. Under optimal conditions, Boc-L-Trp with a series of different concentrations was added in mobile phase and loaded into the MIP- or NIP-coated microchannel at ambient temperature, respectively. As shown in Figure 7, the L_t and K_d values for the MIP-coated microchannel were calculated to be 78 $\mu\text{mol/g}$ and 0.51 mM. The K_d value was much smaller than that of 7.40 mM at a MIP monolithic column,⁴⁰ indicating a good capacity for template recognition. As control, the L_t and K_d values for NIP-coated microchannel were calculated to be

Table 2. Separation Reproducibility and Stability of MIP-MCMD for Boc-Trp Enantiomers at 1 mM ($n = 3$) under Optimal Conditions

analytes	RSD (%) of t_M			RSD (%) of A_p		
	run-to-run	day-to-day	chip-to-chip	run-to-run	day-to-day	chip-to-chip
Boc-D-Trp	1.0	2.5	3.3	1.5	4.3	5.6
Boc-L-Trp	1.2	3.2	3.6	2.1	6.7	8.8

**Figure 7.** Plots of $1/[C(V - V_0)]$ vs $1/C$ for Boc-L-Trp-imprinted and nonimprinted polymer modified capillaries.**Figure 8.** Linear calibration curves for Boc-D-Trp and Boc-L-Trp under optimal conditions.

74 $\mu\text{mol/g}$ and 1.38 mM. The K_d value was higher than that of the MIP-coated microchannel, indicating the imprinted capillary had higher binding affinity for the template than nonimprinted capillary.

Detection of Boc-Trp Enantiomers. The amperometric detection of Boc-Trp enantiomers with a carbon fiber microdisk electrode at +1.2 V (vs Ag/AgCl) showed the linear ranges from 75 to 4000 μM for Boc-D-Trp and 400 to 4000 μM for Boc-L-Trp with the relative coefficients of 0.994 and 0.995 and the slopes of 0.0596 and 0.0392 nC/ μM , respectively (Figure 8). The detection limits at the ratio of S/N of 3 were 20 and 140 μM for Boc-D-Trp and Boc-L-Trp, respectively.

The separation reproducibility of Boc-Trp enantiomers was summarized in Table 2. The relative standard deviations (RSDs) of migration times of Boc-D-Trp and Boc-L-Trp ($n = 3$) were 1.0% and 1.2% for run-to-run, 2.5% and 3.2% for day-to-day, and 3.3% and 3.6% for chip-to-chip, respectively. Thus, the proposed method had good reproducibility and stability. The RSDs of peak area (A_p) measured at the concentration of 1.0 mM analytes ($n = 3$) were 1.5% and 2.1% for run-to-run, 4.3% and 6.7% for day-to-day, and 5.6% and 8.8% for chip-to-chip, respectively, indicating that the MIP-MCMD had good fabrication reproducibility.

CONCLUSIONS

In this work, MIT was introduced into MCE for fast enantioseparation of chiral compounds. The MIP was in situ polymerized on the inner wall of a microchannel using AM as a functional monomer and EDMA as a cross-linker without any need for immobilization of MIP particles. The polymer film linked to the inner wall was highly porous, which provided efficient interaction between the analytes and the MIP. Under optimal separation conditions, the efficient molecular recognition to Boc-Trp enantiomers was achieved in the MIP-MCMD, leading to baseline enantioseparation and good analytical reproducibility and stability. Compared with conventional molecular imprinting analysis, the MIP-MCMD showed highly selective recognition, shortened analytical time, and low reagent and sample consumption. The proposed method of MIP-MCMD provided a promising way for in situ molecular imprinting of a microchannel on a microfluidic device and showed a potential for high-throughput analysis of chiral compounds.

ACKNOWLEDGMENT

We gratefully acknowledge the financial support of the National S&T Pillar Program (Grants 2007BAK26B06 and 2006BAK09B05) and the National Basic Research Program of China (Grant 2010CB732400) from the Ministry of S&T, the National Science Fund for Creative Research Groups (Grant 20821063), the Key Program (Grant 20535010), the Major Research Plan (Grant 90713015), and the General Program (Grants 20875044 and 20705012) from NSFC.

Received for review August 4, 2009. Accepted October 21, 2009.

AC902201A